

# Exploring the role of connectivity in disordered system

Anjan Daimari, Shivaneer Borah, and Diana Thongjaomayum\*

*Department of Physics, Tezpur University, Assam, India, 784028*

(Dated: March 19, 2026)

We study a minimal model of disordered systems, the random field Ising model (RFIM) on a generalized Petersen Graph,  $GP(N, k)$ . This graph has a connected inner and outer loop, where both the loops consist of  $N$  nodes constituting a total of  $2N$  nodes. The parameter  $k$  satisfies the condition  $1 \leq k \leq N/2$ , such that any site  $i$  in the inner loop has  $i - k$  and  $i + k$  as its two nearest neighbours, apart from its connection to a node on the outer loop. Thus, each node in  $GP(N, k)$  has coordination number  $z = 3$ , and by varying  $k$  different connections between the nodes in the inner loop can be obtained. The objective is to study whether different connectivity between nodes in these graphs affects the system's response to an external field when the coordination number is fixed. This is of interest because critical behaviour is absent for  $z \leq 3$  on a random graph which has been solved exactly as well as on the honeycomb lattice in the context of RFIM. Using single-spin-flip Glauber dynamics at zero temperature, we compare the system's response with the known case of a  $z = 3$  random graph and the generalized Petersen graph for various connectivity  $k$ , albeit for the same  $z$ . Our study finds the absence of critical behaviour on  $GP(N, k)$  highlighting the importance of coordination number over varying connectivity between the nodes. Additionally, we explore the case of directed  $GP(N, k)$  and compare it with the undirected  $GP(N, k)$  results.

## I. INTRODUCTION

The nonequilibrium Random Field Ising Model (RFIM) has been extensively studied for understanding disordered spin systems, phase transitions and critical phenomena[1–9]. RFIM has also been experimentally realized in a large number of real materials, such as diluted dipolar magnet, diluted antiferromagnets, single ferroelectric crystals and molecular magnets [10–16], most recently on an artificial spin ice system [17].

The nonequilibrium zero temperature RFIM has been studied on various lattices to understand the role of dimensionality and coordination number in the system's response to slowly varying external field [5, 6, 8, 9]. Studies on random graphs show critical hysteresis for  $z \geq 4$ , whereas critical hysteresis is not observed for  $z \leq 3$ [2]. This shows that  $z$  plays a crucial role in controlling the critical behavior of the system. In quasi-one-dimensional systems, magnetization does not exhibit jump discontinuities, suggesting that dimensionality and connectivity play a significant role in the determination of critical phenomena[18]. Similarly, studies on diluted triangular lattices report that reduced coordination leads to altered phase transition behavior, indicating that lattice structure is a major determinant of disorder induced phenomena [19].

In this study we apply nonequilibrium zero temperature RFIM to  $GP(N, k)$ .  $GP(N, k)$  is a class of structured finite graphs that consists of connected inner and outer loops with  $N$  nodes in each loop, first introduced by Coxeter [20], shown in FIG.1.  $k$  is a parameter with the condition  $1 \leq k \leq N/2$  such that any site  $i$  in the inner loop has  $i - k$  and  $i + k$  as its two nearest neighbors apart from the fixed connection to node,  $i - N$ , of

the outer loop whose other two neighbors are the adjacent nodes to the site:  $(i - N) - 1$  and  $(i - N) + 1$ . By changing the value of  $k$ , different graphs can be obtained [20, 21]. Since its inception,  $GP(N, k)$  has gained immense interest and has been intently studied and analyzed to explore its practical applications like modeling of chemical isomerism[22–25] and designing of interconnection network [26, 27].

By varying  $k$ , we can obtain different connectivity in the graph (or different graphs) with fixed  $z = 3$ . Our main objective is to examine whether the system exhibits interesting trends in magnetization or critical phenomena such as jump discontinuities. We find that  $GP(N, k)$  shows hysteresis and does not exhibit critical behavior. The magnetization curves corresponding to small values of  $\sigma$  for all  $k$  spreads out. However, the magnetization curves for all values of  $k$  collapse onto each other with increasing  $\sigma$ . Furthermore, we also study the directed version of  $GP(N, k)$ .

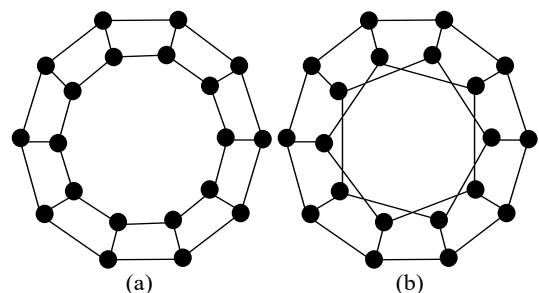


FIG. 1. Schematic representation of  $GP(N, k)$ : (a)  $GP(10, 1)$  and (b)  $GP(10, 2)$ .  $k$  determines how nodes in the inner loop are connected in  $GP(N, k)$ .

\* dianat@tezu.ernet.in

## II. THE MODEL

We consider  $GP(N, k)$ , where each node ( $i = 1, 2, 3, \dots, 2N$ ) is assigned an Ising spin  $S_i = \pm 1$ . Each spin interacts with  $z$  nearest neighboring spins with ferromagnetic interaction strength  $J > 0$ . The system experiences a uniform external field  $h$  and a random field  $h_i$  at each site  $i$ , sampled from a Gaussian distribution with mean,  $\mu = 0$  and standard deviation  $\sigma$ . The random fields are quenched throughout the system's evolution, whereas the spins  $S_i$  evolve. This system corresponds to the Random Field Ising Model [28], and is defined by the Hamiltonian:

$$H = -J \sum_{\langle i, j \rangle} S_i S_j - \sum_i h_i S_i - h \sum_i S_i \quad (1)$$

We employ single spin flip Glauber dynamics at zero temperature in discrete time steps  $t$  [29]:

$$S_i(t+1) = \text{sign} \left[ J \sum_j S_j(t) + h_i + h \right] \quad (2)$$

Here, the summation on the right-hand side is taken over all the  $z$  nearest neighbors associated to the site  $i$ . The system lowers its energy iteratively until it reaches a stable fixed point  $S_i^*(h)$ , for a fixed external field  $h$ . Thus,  $S_i^*(h)$  for each site  $i$ :

$$S_i^*(h) = \text{sign} \left[ J \sum_j S_j^*(h) + h_i + h \right] \quad (3)$$

The system reaches a stable fixed point when all the spins orient in the same direction as their respective local fields for the fixed  $h$ . We begin with an adequately large negative  $h$ , to set the initial configuration of all the spins  $S_i(h = -\infty) = -1$ . Next, the external field  $h$  is gradually varied until a spin loses its stability. At this point the external field is fixed, and subsequently the system is allowed to evolve iteratively until it converges to new fixed point. This new fixed point is termed as the magnetization per site,  $m(h)$ . The  $m(h)$  for the total  $2N$  sites is characterized by:

$$m(h) = \frac{1}{2N} \sum_i S_i^*(h) \quad (4)$$

We then slowly and minimally vary the external field  $h$  such that the next unstable spin flips. This process yields the lower hysteresis  $m_l(h)$ , when  $h$  is ramped up from  $h = -\infty$  to  $+\infty$ . Similarly, when  $h$  is swept from  $h = +\infty$  to  $-\infty$ , we obtain the upper hysteresis  $m_u(h)$ .

$$m_u(h) = -m_l(-h) \quad (5)$$

## III. RESULTS

FIG. 2 shows the hysteresis loops of  $GP(N = 49999, k = 1)$  for different disorder strengths,  $\sigma =$

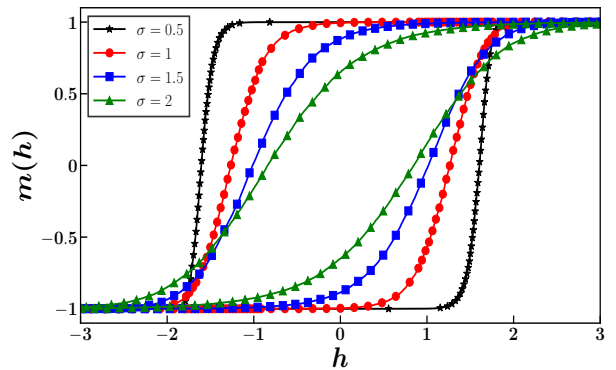


FIG. 2. Hysteresis loops  $m(h)$  vs  $h$  on  $GP(N = 49999, k = 1)$  for different disorder strength  $\sigma$ . Solid line with stars, circles, squares and triangles correspond to  $\sigma = 0.5, 1, 1.5$  and  $2$ , respectively. The  $m(h)$  curves varies smoothly for all the values of  $\sigma$  and the hysteresis loops become narrower with increasing  $\sigma$ .

$0.5, 1, 1.5$  and  $2$ . We observe that the magnetization curves of  $GP(N, k)$  for all the values of  $k$  vary smoothly irrespective of  $\sigma$ . We find no critical value of  $\sigma$  however, as  $\sigma$  increases, the hysteresis loops become narrower. Since the hysteresis behavior is uniform both in the lower and upper loops, we consider only the lower loop of the hysteresis loop. We also observe that the magnetization curves for all the values of  $k$  corresponding to small values of  $\sigma$  spread out. This is shown in the main plot of FIG. 3. However with increasing  $\sigma$ ,  $m(h)$  curves for all values of  $k$  tend to overlap with each other as shown in the inset of FIG. 3. As the coordination number of  $GP(N, k)$  is  $3$ , we also compare our results with the results of RFIM on  $z = 3$  random graph. We observe that for small values of  $\sigma$  the  $m(h)$  curves of  $GP(N, k)$  do not match the results of random graph  $z = 3$ , shown in the main plot of FIG. 3. However, for larger values of  $\sigma$  the  $m(h)$  curves of  $GP(N, k)$  overlap onto the  $m(h)$  curve of random graph  $z = 3$ . We compare the same with the existing analytical results of the random graph [2]. We take the value of  $k = 10$  for the comparison, because the  $m(h)$  curves corresponding to  $k \geq 5$  collapse onto the  $m(h)$  curve of the random graph  $z = 3$  faster with increasing  $\sigma$ . We find that the simulation results of the  $GP(N, k)$  matches exactly with analytical results for higher values of  $\sigma$ , shown in FIG. 4.

The two-leg ladder with periodic conditions [18], and the  $GP(N, 1)$  has the same connectivity and lattice structure. Therefore, we compare the results of  $GP(N, 1)$  with the numerical and analytical results of two-leg ladder. We find that the numerical and analytical of results two-leg ladder match perfectly with the  $GP(N, 1)$  results, though not presented here. The integrated avalanche size distribution  $P(s)$  for  $k = 1, 2, 3, 4, 5, 10, 1000$  and  $10000$  is shown in FIG. 5. We observe that the avalanche size distribution deviates from the power law and bends down spanning only few decades. This characteristic be-

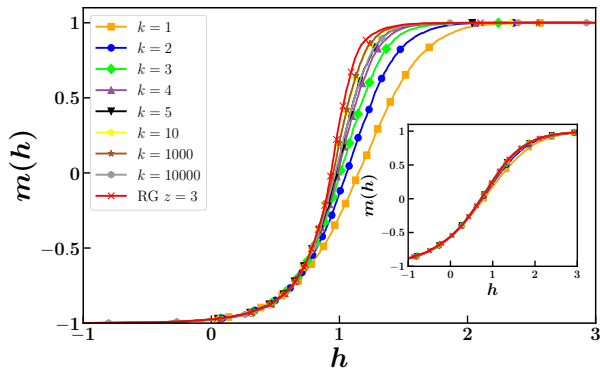


FIG. 3. Plot of  $m(h)$  vs  $h$  on random graph with  $z = 3$  and  $GP(N, k)$  for  $k = 1, 2, 3, 4, 5, 10, 1000$  and  $10000$ . The main plot and inset show results for  $\sigma = 1.2$  and  $\sigma = 2.2$  respectively. The  $m(h)$  curves of  $GP(N, k)$  for different values of  $k$  spread out for small  $\sigma$  values, while  $m(h)$  curves gradually approaches the  $m(h)$  curve of random graph and collapses onto each other for larger  $\sigma$  values. The simulation data is obtained on  $N = 10^6$  for random graph and  $N = 499999$  for  $GP(N, k)$ .

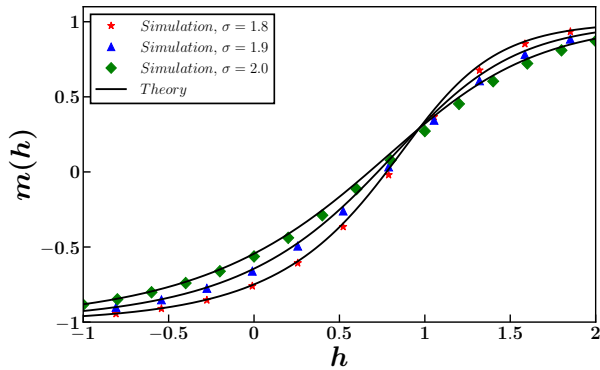


FIG. 4. Comparison of  $m(h)$  vs  $h$  curves obtained from simulation on  $GP(N = 499999, k = 10)$  and analytical solution for  $\sigma = 1.8, 1.9$  and  $2.2$ . The solid lines in the plot correspond to the theoretical predictions and the markers correspond to the simulation results.

haviour supports that  $GP(N, k)$  does not exhibit critical response[30].

Additionally, we extend our study by implementing directed versions of  $GP(N, k)$ . We direct the nodes connecting the outer and inner loops of  $GP(N, k)$ . In other words, the nodes on outer loop consider the interaction from the corresponding nodes at the inner loop, however, the inner nodes interact only with the two other nodes defined by the parameter  $k$  in the inner loop. Initially we consider two types of directed  $GP(N, k)$ , where we uniformly direct the nodes of outer loop towards the inner loop, and vice-versa. Furthermore, we also randomly choose the nodes from the outer or inner loop to be directed towards the outer loop if chosen from inner loop and towards the inner loop if chosen from the outer loop.

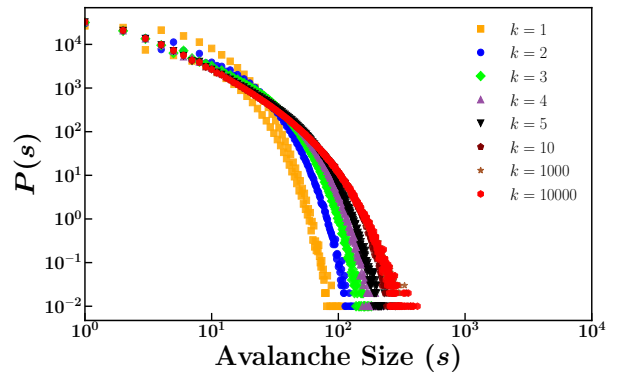


FIG. 5. Log-log plot of the integrated avalanche size distribution for  $k = 1, 2, 3, 4, 5, 10, 1000$  and  $10000$ . The data is obtained on  $GP(N = 499999, k)$  for  $\sigma = 1.2$  averaged over 100 independent configurations. The avalanche size distribution for different values of  $k$  deviates from power law.

The results are the same for all the directed versions of  $GP(N, k)$  studied here and therefore we consider only one result for our analysis. We compare the hysteresis loops of the directed version of  $GP(N, k)$  and  $GP(N, k)$ . We observe that the hysteresis loop of directed  $GP(N, k)$  is narrower compared to the hysteresis loop of  $GP(N, k)$ , see FIG. 6. This owes to the fact that directed  $GP(N, k)$  consists of the outer nodes with  $z = 3$  and inner nodes with  $z = 2$ .

The directed  $GP(N, k)$  also does not exhibit critical behavior like its undirected counterparts. We also find that  $m(h)$  curves of directed  $GP(N, k)$  corresponding to small values of  $\sigma$  for different values of  $k$  do not fully overlap onto each other, shown in the main plot of FIG. 7. However, with increasing  $\sigma$  the  $m(h)$  curves gradually overlap each other, shown in inset of FIG. 7. Similar to  $GP(N, k)$  the integrated avalanche size distribution of directed  $GP(N, k)$  deviates from power law. This is shown in FIG. 8.

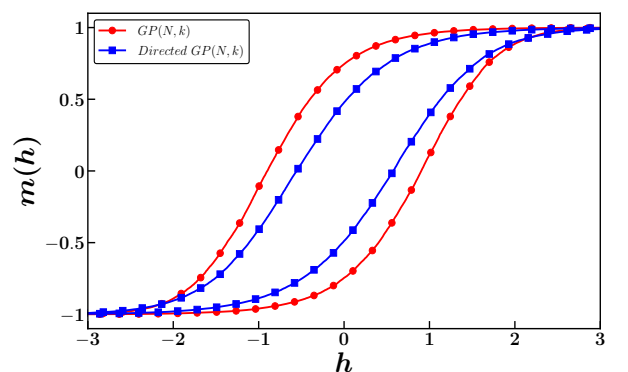


FIG. 6. Comparison of hysteresis loops for undirected and directed  $GP(N, k)$ . The hysteresis loop of directed  $G(N, k)$  shown in blue solid line with squares shows narrower hysteresis. The simulation data is obtained for  $N = 499999, k = 1$  and  $\sigma = 1.8$ .

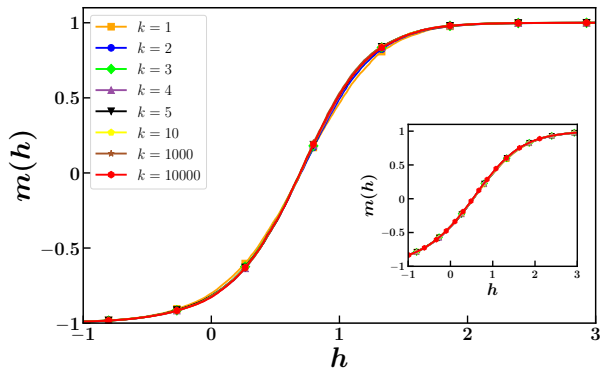


FIG. 7. Plot of  $m(h)$  vs.  $h$  on the directed  $GP(N = 499999, k)$  for  $k = 1, 2, 3, 4, 5, 10, 1000$  and  $10000$ . The main plot and inset show results for  $\sigma = 1.2$  and  $\sigma = 2$  respectively. The  $m(h)$  curves for different values of  $k$  do not completely overlap for small values of  $\sigma$ , however with increasing  $\sigma$ , the curves tend to align perfectly onto each other.

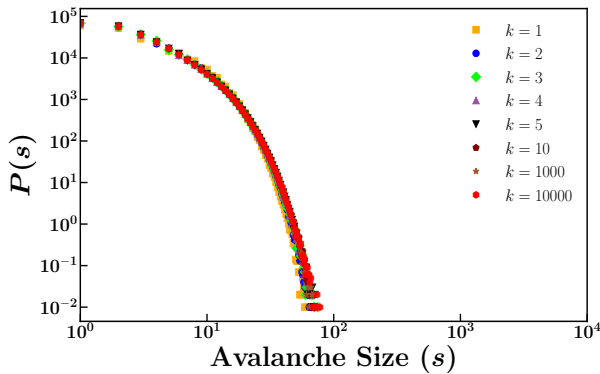


FIG. 8. Log-log plots of integrated avalanche size distribution for  $k = 1, 2, 3, 4, 5, 10, 1000$  and  $10000$ . The data is obtained on directed  $GP(N = 499999, k)$  for  $\sigma = 1.2$  averaged over 100 independent configurations. Similar to the undirected version of  $GP(N, k)$ , in the directed  $GP(N, k)$  the avalanche size distribution for different values of  $k$  shows bending down and does not span for many decades.

## IV. CONCLUSION

In summary, we have presented the numerical results of the zero temperature RFIM on  $GP(N, k)$ . We find that  $GP(N, k)$  and directed  $GP(N, k)$  show hysteresis but do not exhibit critical behavior, which is consistent with the finding on  $z = 3$  random graph [2]. The  $m(h)$  curves of  $GP(N, k)$  corresponding to small values of disorder  $\sigma$  are spread out irrespective of the  $k$  value. However, on increasing  $\sigma$  the curves merge onto one other. The same behaviour is observed in the case of directed  $GP(N, k)$ . The results of  $GP(N, k)$  are consistent with the numerical and analytical results of  $z = 3$  random graph for higher values of  $\sigma$ . This ensures the availability of exact solution on the GP in the limit of large disorder. The avalanche size distribution for both the  $GP(N, k)$  and directed  $GP(N, k)$  does not span for many decades and bends faster which is another signature of system showing no critical response[30].

This is the first report of RFIM on Generalised Petersen Graph. The importance of coordination number rather than how the connectivity is established, is highlighted in the present study. The propagation of large avalanche requires a minimum connectivity to facilitate the critical response. Hence, graphs or regular lattices with  $z > 3$  show critical behaviour in the context of nonequilibrium RFIM. The study of graphs is crucial not only from the mathematical aspect, but also from the perspective of network studies.

## ACKNOWLEDGEMENTS

AD and DT acknowledge the Department of Science and Technology, Anusandhan National Research Foundation, ANRF (Then DST-SERB), Government of India, for financial support under POWER Grant No. SPG/2022/000678. DT also acknowledges partial support from ANRF PAIR Grant No. ANRF/PAIR/2025/000029/PAIR.

- 
- [1] J. P. Sethna, K. Dahmen, S. Kartha, J. A. Krumhansl, B. W. Roberts, and J. D. Shore, *Physical Review Letters* **70**, 3347 (1993).
  - [2] D. Dhar, P. Shukla, and J. P. Sethna, *Journal of Physics A: Mathematical and General* **30**, 5259 (1997).
  - [3] S. Sabhapandit, P. Shukla, and D. Dhar, *Journal of Statistical Physics* **98**, 103 (2000).
  - [4] J. P. Sethna, K. Dahmen, and C. R. Myers, *Nature* **410**, 242 (2001).
  - [5] R. S. Kharwanlang and P. Shukla, *Physical Review E* **85** (2012).
  - [6] P. Shukla and D. Thongjaomayum, *Journal of Physics A: Mathematical and Theoretical* **49**, 235001 (2016).
  - [7] P. Shukla and D. Thongjaomayum, *Physical Review E* **95**, 042109 (2017).
  - [8] D. Thongjaomayum and P. Shukla, *Physical Review E* **99**, 062136 (2019).
  - [9] S. Mijatović, D. Jovković, and D. Spasojević, *Physical Review E* **103**, 032147 (2021).
  - [10] S. Fishman and A. Aharony, *Journal of Physics C: Solid State Physics* **12**, L729 (1979).
  - [11] J. Hill, Q. Feng, R. Birgeneau, and T. Thurston, *Zeitschrift für Physik B Condensed Matter* **92**, 285 (1993).
  - [12] M. Schechter, *Physical Review B—Condensed Matter and Materials Physics* **77**, 020401 (2008).

- [13] S. Miga, W. Kleemann, J. Dec, and T. Lukasiewicz, *Physical Review B—Condensed Matter and Materials Physics* **80**, 220103 (2009).
- [14] V. Westphal, W. Kleemann, and M. Glinchuk, *Physical Review Letters* **68**, 847 (1992).
- [15] A. Millis, A. Kent, M. Sarachik, and Y. Yeshurun, *Physical Review B—Condensed Matter and Materials Physics* **81**, 024423 (2010).
- [16] J. Xu, D. Silevitch, K. Dahmen, and T. Rosenbaum, *Physical Review B* **92**, 024424 (2015).
- [17] N. Bingham, S. Rooke, J. Park, A. Simon, W. Zhu, X. Zhang, J. Batley, J. Watts, C. Leighton, K. Dahmen, *et al.*, *Physical review letters* **127**, 207203 (2021).
- [18] S. Sabhapandit, *Physical Review B—Condensed Matter and Materials Physics* **70**, 224401 (2004).
- [19] L. Kurbah, D. Thongjaomayum, and P. Shukla, *Physical Review E* **91**, 012131 (2015).
- [20] H. S. Coxeter, *Bulletin of the American Mathematical Society* **56**, 413 (1950).
- [21] M. E. Watkins, *Journal of Combinatorial Theory* **6**, 152 (1969).
- [22] K. Balasubramanian, *Journal of Mathematical Chemistry* , 1 (2025).
- [23] H. Raza, J.-B. Liu, M. Azeem, and M. F. Nadeem, *Complexity* **2021**, 5592476 (2021).
- [24] K. Mislow, *Accounts of Chemical Research* **3**, 321 (1970).
- [25] A. J. Schwenk, *Journal of Combinatorial Theory, Series B* **47**, 53 (1989).
- [26] M. S. Krishnamoorthy and B. Krishnamurthy, *Computers & Mathematics with Applications* **13**, 577 (1987).
- [27] G. B. Ekinici and J. B. Gauci, *Discrete Applied Mathematics* **252**, 2 (2019).
- [28] T. Nattermann, *Spin Glasses and Random Fields* , 277 (1998).
- [29] R. J. Glauber, *Journal of Mathematical Physics* **4**, 294 (1963).
- [30] C. L. Farrow, P. Shukla, and P. M. Duxbury, *Journal of Physics A: Mathematical and Theoretical* **40**, F581 (2007).